New cholesterol-specific antibodies remodel HIV-1 target cells' surface and inhibit their in vitro virus production

Zoltán Beck,[1,*] Andrea Balogh,[1,†] Andrea Kis,* Emese Izsépi,[†] László Cervenak,[§] Glória László,[†] Adrienn Bíró,** Károly Liliom,[††] Gábor Mocsár,[§§] György Vámosi,[§§] George Füst,[§] and Janos Matko[3,†,***]

Institute of Medical Microbiology,* University of Debrecen, H-4012, Debrecen, Hungary; Department of Immunology[†] and Immunology Research Group of Hungarian Academy of Sciences,*** Eötvös Loránd University, H-1117, Budapest, Hungary; Research Group of Immunogenomics,[§] Hungarian Academy of Sciences at Semmelweis University, H-1089, Budapest, Hungary; Research Laboratory,** 3rd Department of Internal Medicine, Semmelweis University, H-1125, Budapest Hungary; Institute of Enzymology,[††] Biological Research Center, Hungarian Academy of Sciences, H-1518, Budapest, Hungary; and Cell Biology and Signaling Research Group of the Hungarian Academy of Sciences,[§§] Department of Biophysics and Cell Biology, Research Center for Molecular Biology, University of Debrecen, H-4012, Debrecen, Hungary

Abstract The importance of membrane rafts in HIV-1 infection is still in the focus of interest. Here, we report that new monoclonal anticholesterol IgG antibodies (ACHAs), recognizing clustered membrane cholesterol (e.g., in lipid rafts), rearrange the lateral molecular organization of HIV-1 receptors and coreceptors in the plasma membrane of HIV-1 permissive human T-cells and macrophages. This remodeling is accompanied with a substantial inhibition of their infection and HIV-1 production in vitro. ACHAs promote the association of CXCR4 with both CD4 and lipid rafts, consistent with the decreased lateral mobility of CXCR4, while Fab fragments of ACHAs do not show these effects. ACHAs do not directly mask the extracellular domains of either CD4 or CXCR4 nor do they affect CXCR4 internalization. No significant inhibition of HIV production is seen when the virus is preincubated with the antibodies prior to infection. Thus, we propose that the observed inhibition is mainly due to the membrane remodeling induced by cholesterol-specific antibodies on the target cells. This, in turn, may prevent the proper spatio-temporal juxtaposition of HIV-1 glycoproteins with CD4 and chemokine receptors, thus negatively interfering with virus attachment/entry.—Beck, Z., A. Balogh, A. Kis, E. Izsépi, L. Cervenak, G. László, A. Bíró, K. Liliom, G. Mocsár, G. Vámosi, G. Füst, and J. Matko. **New cholesterol-specific antibodies remodel HIV-1 target cells' surface and inhibit their in vitro virus production.** *J. Lipid Res.* 2010. 51: 286–296.

Anticholesterol antibodies (ACHAs) naturally occur in the sera of most healthy individuals with yet unknown functions (1). Recently, we reported on new IgG-type monoclonal antibodies, AC1 and AC8, which are highly specific to clustered cholesterol and some 3β-OH-containing sterols and do not cross-react with other lipids (2). These antibodies, in contrast to the IgM-type ACHAs reported earlier, have a unique property of spontaneous binding to live phagocytes and T-cells. Furthermore, their binding to the cell surface was substantially sensitive to the epitope accessibility, e.g., it was greatly enhanced by limited papain digestion of membrane proteins with long extracellular domains. Their spontaneous binding to intact cells also showed cell-type dependence. The preferential binding sites for these new cholesterol-specific mAbs were identified as cell surface or intracellular membrane compartments enriched in clustered cholesterol, such as lipid rafts, caveolas, or Golgi complexes (2).

Lipid rafts are dynamic, glycosphingolipid-, and cholesterol-rich membrane microdomains considered to make "some order into the chaos" of biological membranes (3, 4). Many pieces of experimental evidence indicate that the human immunodeficiency virus type 1, HIV-1, enters target cells through these lipid rafts (5–7). The last stage of

[1] Z. Beck and A. Balogh contributed equally to this work.
[2] Present address of Z. Beck: U.S. Military HIV Research Program, Henry M. Jackson Foundation for the Advancement of Military Medicine, Walter Reed Army Institute of Research, Rockville, MD 20850
[3] To whom correspondence should be addressed.
  e-mail: matko@elte.hu

This article is available online at http://www.jlr.org

the multistep process of HIV-1 entry, the fusion of the virus with the target cell membrane, entails multifocal interactions between virus shell glycoproteins and lipids and their receptor/coreceptor and lipid raft counterparts on target cells (8). Lipid rafts were also implicated in the budding of the progeny virus (9, 10).

HIV-1 was shown to use the CD4 receptor and CCR5 or CXCR4 chemokine receptors for productive entry into $CD4^+$ cells. CD4 and CCR5 are constitutively raft associated, while CXCR4 molecules are mostly recruited to lipid rafts after the initial binding of the virus (11). However, the exact molecular mechanism of this entry is still under debate (9, 12). Since the new cholesterol-specific mAbs selectively bind to cholesterol-enriched lipid raft or caveola microdomains of intact HIV-1 permissive cells, it is plausible to assume that they may interfere somehow with the mechanisms leading to membrane attachment or internalization of the virus.

Therefore, this study aimed to investigate whether the new ACHAs can modulate the receptor or microdomain architecture at the surface of target cells, such as human macrophages and T-cells: namely, the distribution/interaction pattern, accessibility, internalization, mobility, or raft association of CD4 and chemokine receptors. These properties are all critical for membrane attachment and internalization of the virus.

Since in a recent work (13) another antilipid antibody, a mAb against phosphatidylinositol-4-phosphate, was reported to inhibit infection of peripheral blood mononuclear cells (PBMCs) with two HIV-1 primary isolates, we also investigated whether the new cholesterol-specific antibodies can affect in vitro HIV-1 infection/production of primary monocyte-derived macrophages (MDMs) and T-cells in cultures.

The new IgG-type cholesterol-specific antibodies caused a remarkable lateral clustering of membrane rafts upon binding to both cell types and remodeled the interaction pattern of CXCR4 chemokine receptors with both CD4 and lipid rafts. The membrane-bound antibodies substantially inhibited production of two different HIV strains in MDM and T-cells in vitro. In contrast, no significant inhibition was achieved when the virus strains themselves were preincubated with the antibodies before infection. Thus, these data demonstrate a novel type of inhibition of HIV-1 infection by lipid (cholesterol)-specific mAbs, which is linked to their primary membrane remodeling effect on target cells. This, in turn, can prevent the efficient multistep virus anchorage.

MATERIALS AND METHODS

Cells, immunofluorescence labeling, and flow cytometry

The monoclonal IgG_3 Abs to cholesterol, AC1 and AC8, were generated, characterized, and applied for cell labeling as described previously (2). Cell surface binding of Alexa488-ACHA, PE/Cy5-anti-CD4 (ImmunoTools, Friesoythe, Germany), or APC-anti-CXCR4 (R and D Systems, Minneapolis, MN) was assayed by flow cytometry. After FcR blocking with affinity-purified human

IgG_1, cells were washed with FACS (fluorescence activated cell analysis and sorting) buffer containing 0.1% BSA and then stained as described elsewhere (2). Occasionally, prior to receptor staining, U937 human macrophages (ATTC, maintained in RPMI 1640 medium + 10% FBS) and MT-4 T-cells were preincubated with ACHA or the Ka40 isotype control Ab (specific to tobacco mosaic virus) at 37°C for 60 min.

In the CXCR4 receptor internalization assay, U937 cells were incubated (or not) with ACHA as described above. After washing, cells were treated with 300 nM SDF-1α chemokine ligand or, alternatively, with 100 ng/ml of the phorbol ester PMA, at 37°C, for 0–60 min. Cells were then washed, FcR-blocked, and labeled with APC-anti-CXCR4 as described above. Before measurement, cells were fixed with 3% paraformaldehyde. CXCR4 expression on the cell surface was measured and evaluated by flow cytometry.

Data from 10,000 stained cells/sample were acquired in a Becton-Dickinson FACSCalibur flow cytometer using CellQuest Pro software (Becton-Dickinson, San Jose, CA) and then analyzed with FCS3 Express software (De Novo Software, Los Angeles, CA).

Surface plasmon resonance

Surface plasmon resonance measurements were performed using a BIACORE X instrument (Biacore, Uppsala, Sweden) at 25°C. AC8 ACHA and anti-CD8 control IgG (30 μg/ml) were immobilized onto the surface of a carboxymethylated dextran chip (CM5) using standard amine-coupling chemistry in 10 mM sodium acetate, pH 5.0, according to the manufacturer's instructions. The mean amount of immobilized protein was ∼7000 resonance units. Cholesterol-rich (1,2-dimiristoyl-*sn*-glycero-3-phosphocholine, 1,2 dimiristoyl-*sn*-3-phosphoglyerol and cholesterol, in a 9:1:25 molar ratio) and cholesterol-free control liposomes were prepared as described earlier (2), reconstituted in 10 mM HEPES, pH 7.2, 150 mM NaCl solution (running buffer) at a concentration of 1 mM total lipid, and were passed over the chip surface at a flow rate of 10 μl/min. The results were analyzed by BIAevaluation 4.1 software (Biacore). The corresponding association and dissociation regimes of sensorgrams were fitted to a builtin Langmuir binding model, and the equilibrium dissociation constant, K_D, was calculated as the ratio of dissociation to association rate constants.

Confocal microscopy

U937 human macrophages were treated with AC8 (or Ka40 isotype control) antibodies as described above and, as a negative control to raft-associated proteins, with anti-CD71 (transferrin receptor) mAb (MEM-75; a kind gift from Vaclav Horejsi, Prague, CZ). Alternatively, cells were treated with monovalent Fab fragment of AC8 IgG, generated by the method of Adamczyk (14). The enzyme reaction was stopped by adding iodoacetamide, the digested protein was separated on Sephadex G-100 column (Pharmacia Fine Chemicals, Uppsala, Sweden), and the homogeneity of the Fab-containing fractions was analyzed by SDS gel electrophoresis.

Cells were then washed, FcR blocked, and stained with fluorophore-conjugated anti-CD4, anti-CXCR4, and Alexa488- or Alexa647-CTX (Invitrogen-Molecular Probes, Eugene, OR) in different combinations. After washing and fixing in 3% paraformaldehyde, labeled cells were mounted on quartz-glass bottomed microplates (Lab-Tek, Nalge Nunc, Rochester, NY) and assayed with an Olympus Fluoview 500 confocal microscope (Hamburg, Germany) equipped with four optical channels, using a 60× (numerical aperture of 1.45) oil immersion objective.

Colocalization indices were determined from ≥100 cells (∼200 regions of interest/sample, in four independent experi-

ments) by ImageJ software (http://rsbweb.nih.gov/ij) using the appropriate colocalization plug-in. The Pearson's colocalization index (CI) provides a reliable estimate on the extent of protein colocalization: CI values close to zero indicate no or a very low degree, while CI ≥ 0.5 reflects a high degree of colocalization, whereas the CI = 1 value would correspond to a full overlap between the two colors in each pixel of the image (15).

Fluorescence resonance energy transfer

For ratiometric intensity-based fluorescence resonance energy transfer (RiFRET) measurements, U937 macrophages were treated with AC8 or Ka40 isotype control antibodies and stained with Alexa546-conjugated anti-CD4 (donor only sample), with APC-conjugated anti-CXCR4 (acceptor only sample), or with both antibodies as described above. After washing, labeled cells were mounted on quartz-glass bottomed microplates treated with BD Cell-Tak cell and tissue adhesive (Becton-Dickinson), according to the manufacturer's protocol. RiFRET measurements on a pixel-by-pixel basis were performed at room temperature on an Olympus Fluoview 500 confocal microscope using a 60× (numerical aperture of 1.45) oil immersion objective. The Alexa546-conjugated antibody was excited with a 532 nm HeNe laser and detected through a 560–600 nm emission filter, and the Alexa647-labeled protein was excited with a 633 nm HeNe laser and detected through a 660 nm long-pass filter. FRET efficiency was calculated from ≥ 30 cells by the ImageJ RiFRET plugin (16).

Fluorescence correlation spectroscopy

For fluorescence correlation spectroscopy (FCS) measurements, U937 human macrophage cells were treated with AC8 or Ka40 isotype control antibodies and stained with Alexa488-conjugated anti-CD4 or APC-conjugated anti-CXCR4 as described above. As control, cells were labeled with Alexa647-anti-CD2 (Exbio, Praha, CZ) or Alexa488-AC8 antibodies for 30 min on ice. After washing, labeled cells were mounted on quartz-glass bottomed microplates.

FCS (17) measurements were carried out at room temperature, in a fluorescence fluctuation microscope set on an Olympus FluoView 1000 confocal microscope base, with a two-channel FCS extension. Desired points were selected for FCS analysis from confocal sections of the sample. Fluorescence fluctuations were detected by avalanche photodiodes (Perkin-Elmer, Wellesley, MA), and the autocorrelation function was calculated by an ALV-5000E hardware correlator card (ALV Laser, Langen, Germany) in real time. From each sample n > 22 cells were measured, and 10 × 5 s runs were recorded per cell. Data were fitted to a single-component two-dimensional diffusion model with a triplet term using the program QuickFit (written in the laboratory of J. Langowski, DKFZ, Heidelberg, Germany):

$$G(\tau) = \frac{1}{N} \frac{\left(1 - T + Te^{-\tau/\tau_{tr}}\right)}{1 - T} \left[\left(1 + \frac{\tau}{\tau_d}\right)^{-1}\right]$$

where N is the average number of molecules in the detection volume, T is the fraction of dyes being in the triplet state within the detection volume, τ_{tr} is the phosphorescence lifetime, and τ_d is the diffusion time, which is the average time spent by the dye in the detection volume. The half-decay time $\tau_{1/2}$ was used to determine the average diffusion coefficients as described earlier (18).

Target cells and HIV-1 strains

HIV-1$_{IIIB}$ permissive H9 cell line (for virus propagation) and MT-4 T cells (ATCC) were maintained in complete RPMI 1640 medium (cRPMI; 10% FBS, 100 U/ml penicillin, 100 µg/ml streptomycin, and 1 mM L-glutamine; Gibco BRL, Gaithersburg, MD). The primary MDM cells were separated from peripheral blood mononuclear cells of healthy, HIV-1 seronegative donors using PHA stimulation as described earlier (19). The MDM cultures were used for HIV-1 infection in all experiments on day 7 after separation.

The ×4 phenotype IIIB strain of HIV-1 (20) was grown in H9 cell line, while the R5 characteristic Ada-M strain of HIV-1 (19) was propagated in primary MDM cultures, then harvested and stored in liquid nitrogen.

Infection and measurement of HIV-1 production

Different protocols for antibody treatment, infection, and washing prior to virus production measurement were used for assaying with which stage of the HIV-1 infection and virus cycle (attachment, fusion, entry, or budding) the ACHAs interfere. Protocol 1: Prior to infection with the appropriate virus strains, either the target cells or the viruses were pretreated with ACHAs for 60 min at 37°C. Then, the untreated or ACHA-pretreated cells in culture were infected with untreated or ACHA-pretreated virus for 1 h at 37°C. Infection was followed by culturing T-cells or MDM cells for 4 or 14 days, respectively, before measurement of virus production.

Protocol 2: Target cells were treated with the appropriate ACHAs for 1 h at 37°C, infected with HIV-1 strains for 1 h at 37°C, and then washed out carefully (or not). The samples were then left in culture for 4 or 14 days, respectively, before measurement of virus production.

Protocol 3: Since during the assay period a continuous decline of ACHA concentration in the supernatant was observed, a third strategy was applied to investigate ACHA's effects on virus production. Cells were preincubated with ACHAs according to protocol 1, washed, and infected, and a continuous supplementation of ACHA was applied during the 4 or 14 day assay periods to maintain a constant level of ACHAs in the extracellular fluid. This strategy aimed to reveal any effect of the antibodies on the budding phase.

Untreated and Newcastle Disease Virus-specific isotype control antibody treated cells were also used as controls in all infection experiments.

HIV-1 infection was carried out with 100 µl of IIIB or Ada-M strains of HIV-1 with 15,000 cpm reverse transcriptase activity in all protocols. Target cells (in 300 µl cRPMI) were incubated with the virus at 37°C for 60 min, washed (or not) with medium, and then completed up to 1 ml with fresh cRPMI medium.

HIV-1 production was measured by reverse transcriptase assay (21) with a Packard 2200CA TRI-CARB Liquid Scintillation Analyzer (Packard Instrument, Meriden, CT) and corrected to dpm values.

Cellular cytotoxicity assay

MT-4 and MDM cells were treated with different concentrations of ACHA and incubated in the appropriate medium for 4 or 14 days, respectively. Cells were assayed periodically for in vitro cytotoxicity of the ACHAs. Viability of cells was determined by the CellTiter 96® AQ$_{ueous}$ nonradioactive Cell Proliferation Assay (Promega, Madison, WI) (22) according to the manufacturer's protocol. The assay is based on MTT-formazan reaction of metabolically active cells. In each experiment, the survival rate and the standard deviation were calculated from triplicates of samples.
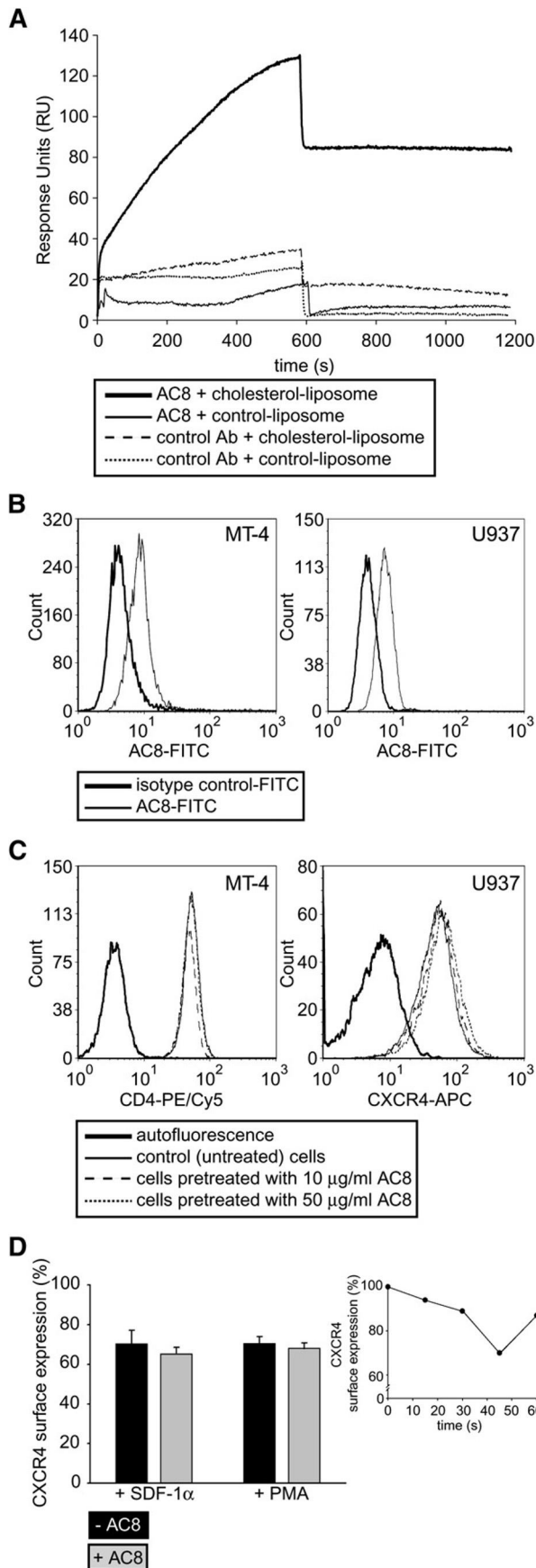
Fig. 1. AC8 mAb bound to HIV-permissive T-cells and macrophages neither masks the accessibility of CD4 and CXCR4 receptors nor affects internalization of CXCR4. A: Surface plasmon

Measurement of anticholesterol antibodies in cell culture supernatants by ELISA

Concentration of anticholesterol antibodies in cell culture supernatants was measured by the ELISA method as described previously (2).

Statistical analysis

Diffusion coefficients in control and ACHA-treated cells were compared using Student's *t*-test (the number of individual cells for each sample is given in Table 1).

RESULTS

Binding properties of ACHAs to cholesterol-rich surfaces assessed by surface plasmon resonance

To quantitate binding of ACHA to highly homogenous cholesterol-rich liposomes used in generating these antibodies (2), as an optimal epitope, we used surface plasmon resonance experiments. AC8 ACHA and anti-CD8 control IgGs were immobilized in different flow channels on the surface of the same CM5 sensor chip. As depicted on the representative binding curves of **Fig. 1A**, liposomal presentation of cholesterol resulted in a significant binding to the AC8 ACHA but not to the anti-CD8 control antibody. Cholesterol-free liposomes exhibited no binding to the IgGs, as expected. The dissociation phase of the binding reaction can be fitted to a single exponential, yielding a dissociation rate, $k_{off} = 1.6 \pm 0.5 \times 10^{-5}\,s^{-1}$ (n = 3). The association phase can be estimated kinetically only if the concentration of the analyte (binding partner in solution) is known. ACHA is expected to interact with the cholesterol-rich liposome as a whole rather than with individual cholesterol molecules. Since the lipid was presented as a 1 mM solution (regarding total lipid concentration), a rough estimate of analyte concentration is 10 µM, assuming ~100 lipids/liposome (based on average liposome size). Using this analyte concentration, the fit yielded an association rate, $k_{on} = 205 \pm 8\,M^{-1}\,s^{-1}$ (n = 3). The equilibrium dissociation constant estimated from these rate constants is $K_d = k_{off}/k_{on} = 78 \pm 27$ nM.

These data, completing recent semiquantitative results showing low/medium affinity ACHA binding to isolated

resonance measurement of the interaction between ACHA and cholesterol-rich liposomes. Liposomal presentation of cholesterol resulted in binding to immobilized AC8 ACHA but not to anti-CD8. Cholesterol-free liposomes exhibited no binding to the IgGs. Fitting of a Langmuir binding model to AC8 data yielded an equilibrium dissociation constant $K_d = k_{off}/k_{on} = 78 \pm 27$ nM. Typical traces of three to four experiments are shown. B: The AC8 antibody spontaneously binds to the surface of MT-4 T and U937 macrophage cells, respectively. C: Flow cytometric histograms of untreated or AC8-treated MT-4 or U937 cells stained with PE/Cy5-anti-CD4 or APC-anti-CXCR4, respectively, are shown. D: SDF-1α or PMA-induced internalization of CXCR4 is shown for untreated or AC8-pretreated U937 cells. Cell surface expression of CXCR4, measured by flow cytometry 45 min after stimulation, is displayed as mean ± SD from three independent experiments. The time course of internalization is also shown in the insert. The expression level of untreated cells was taken as 100%.

membrane raft fractions of T-cells (2), suggest that the optimal affinity of ACHAs to clustered cholesterol is medium, meanwhile the binding is highly selective.

Binding of AC8 does not alter the accessibility or internalization of HIV-1 receptors on target cells

Earlier, we demonstrated the spontaneous binding of the new cholesterol-specific antibodies to several mouse and human lymphoid and myeloid cell types (2). Here, we show that AC8 can also bind to HIV-1 permissive human MT-4 T cells and U937 macrophages (Fig. 1B), the potential target cells of the IIIB and Ada-M HIV-1 strains, respectively. In addition, AC8 does not mask the extracellular domains of CD4 or CXCR4 receptors on these cells, since the binding of antibodies against these epitopes remained unchanged after AC8 binding (Fig. 1C).

The HIV-1 coreceptor CXCR4 was shown to rapidly internalize upon binding chemokine ligand SDF-1α or after PMA treatment, and a mechanism involving the cytoskeleton and motor proteins (myosin IIa) was also proposed for this process (23). It was supposed that internalization of the chemokine receptor may also influence HIV-1 interaction/entry to target cells. Therefore, the SDF-1 or PMA-induced internalization of CXCR4 was also followed in context with the possible effects of the AC8 antibody. Results with human U937 macrophage cells showed that the cholesterol-specific antibody AC8 does not significantly affect internalization of CXCR4 induced either by SDF-1 or PMA (Fig. 1D).

Binding of AC8 to the target cells' surface induces lateral lipid raft clustering

Interestingly, binding of AC8 to U937 macrophages induced several remarkable changes in their global plasma membrane organization. The cell surface ganglioside (GM1-rich raft) pattern was markedly altered as indicated by the increased fraction of highly patchy cells (from 10 to 67%) and the increased average GM1 raft size (from 200–300 nm to 0.5–1 μm in diameter) (**Fig. 2**). Similar changes were observed on T-cells as well (data not shown).

The AC8 antibody remodels the lateral plasma membrane interaction pattern of chemokine receptor CXCR4 with CD4 and lipid rafts on target cells

First, the interaction pattern of CD4 HIV-1 receptor and the CXCR4 coreceptor with each other and with the lipid rafts was investigated in human U937 monocyte-macrophage cells by means of confocal microscopy colocalization analysis. The chemokine receptor CXCR4 colocalized only weakly with CD4 (CI: ~0.2), in accordance with earlier reports on other cells (6, 24), and also moderately (CI: 0.2–0.3) with GM_1 ganglioside rafts marked with fluorescent cholera toxin B subunit. In contrast, the CD4-cholera toxin B subunit colocalization was high (CI: >0.6), similar to many other cell types (**Fig. 3**). This indicates the lack of significant association between CD4 and CXCR4 on these target cells and is also consistent with their localization in distinct membrane microdomains in the absence of the virus.
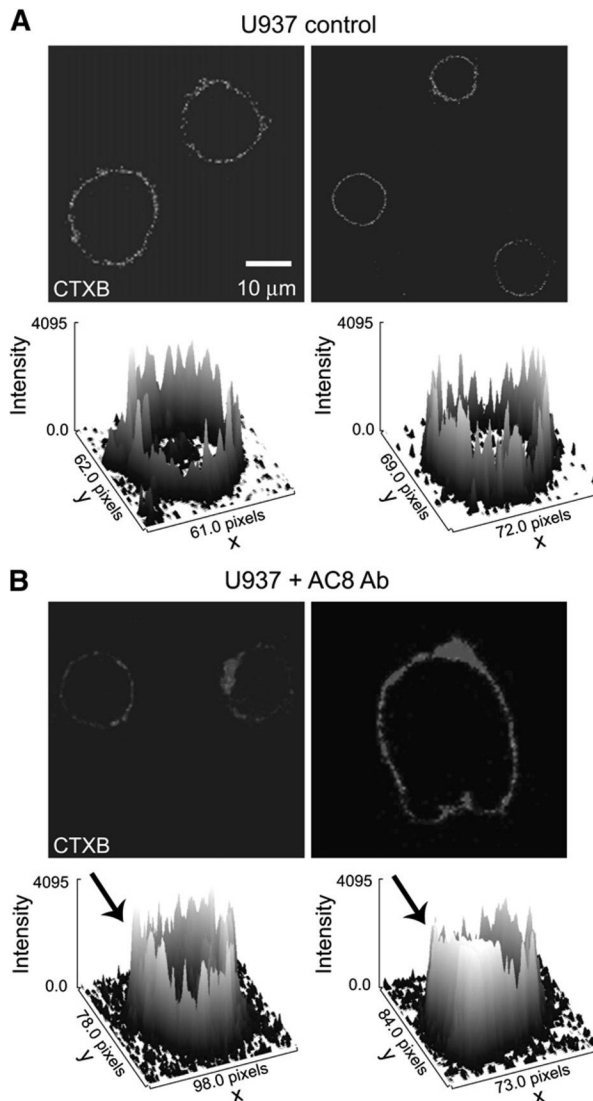
Fig. 2. Binding of monoclonal ACHA to human macrophages alters the size distribution of GM_1-rich rafts. Untreated (A) or ACHA-pretreated (B) U937 cells were stained with Alexa488-cholera toxin B and assayed by confocal microscopy. Representative images and surface intensity plots reflect an AC8-induced microaggregation/coalescence (see arrows) of lipid rafts. The average size of GM_1 rafts increased from 200–300 nm to 0.5–1 μm in diameter. Results were obtained evaluating >120 cells from three independent experiments.

Binding of AC8 antibody to these cells caused an ~2-fold increase of the colocalization between CXCR4 and CD4 as well as between CXCR4 and GM_1 rafts, while leaving CD4 raft colocalization unchanged. Neither the engagement/cross-linking of a nonraft protein, the transferrin receptor (CD71) with its specific mAb, nor the isotype control antibody affected these colocalization patterns. The monovalent Fab fragment of AC8 antibody, without cross-binding capacity, had no effect on the colocalization between HIV receptors (**Fig. 4A**).

The increased proximity/interaction between CXCR4 and CD4 was further confirmed by intensity-based FRET measurements. Mean FRET values (±SD) were 0.17 (±0.02)
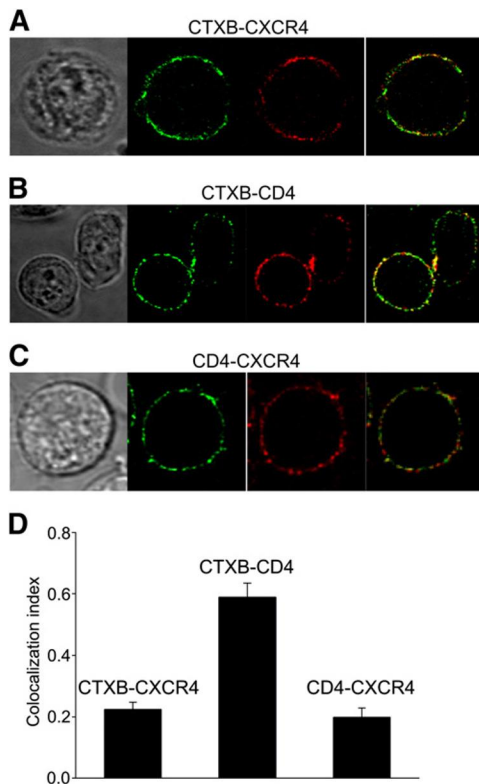
Fig. 3. Colocalization pattern of CD4, CXCR4, and GM₁-enriched lipid rafts in HIV-1 permissive human macrophage cells. Representative confocal images of U937 cells double labeled with Alexa488-cholera toxin B subunit (CTXB) (green) and APC-anti-CXCR4 (red) (A), RPE-anti-CD4 (green) and Alexa647-CTXB (red) (B), and RPE-anti-CD4 (green) and APC-anti-CXCR4 (red) (C) are shown. Colocalization indices for CD4, CXCR4, and CTXB in different combinations (D) were derived from ≥100 cells (~250 regions of interest) of three independent samples and displayed as mean ± SD.

in control cells, while it elevated to 0.28 (±0.06) upon AC8 binding of target cells (Fig. 4B).

The AC8 antibody selectively reduces the lateral mobility of CXCR4 but not that of CD4

In order to see whether AC8 has any influence on the molecular mobility of plasma membrane HIV-1 receptors, the diffusion properties of CXCR4 and CD4 were assessed by FCS imaging. AC8 binding to macrophages significantly reduced two-dimensional diffusion of CXCR4 but not that of CD4 (**Fig. 5A, B**). Diffusion of a nonraft protein, CD2, was not affected by ACHA treatment either in macrophages (Fig. 5C; **Table 1**) or in T-cells (data not shown). The average diffusion coefficient of CXCR4 decreased by ~40% ($P < 0.01$). Fab fragment of AC8 did not show this effect (data not shown). The AC8 mAb bound to the cell membrane diffused remarkably slower (diffusion coefficient, D: 0.2 $\mu m^2/s$) than small fluorescent cholesterol probes (e.g., Bodipy cholesterol) do in model membranes with high cholesterol content (D: 0.5 $\mu m^2/s$) and almost 10-fold slower than cholesterol does in fluid membrane phases (25). This indicates that the cell-surface-bound ACHA diffuses in large molecular clusters (Table 1).

Cholesterol-specific AC1 and AC8 monoclonal antibodies inhibit in vitro HIV-1 production by T-cells and macrophages

Next we investigated whether these substantial changes in the membrane organization of HIV-1 permissive target cell types have any effect on their infection and virus production. First, it was observed that the presence of ACHAs in cell cultures of MT-4 or MDM cells, at the time of infection, resulted in significant inhibition of the virus production of these cells (data not shown). Analyzing the details of this inhibitory effect, cultured MT-4 T-cells and primary MDM cells were preincubated with ACHAs prior to infection with IIIB and Ada-M strains of HIV-1, respectively (see protocol 1 in Materials and Methods). Such preincubation resulted in a significant (up to 50–60%) dose-dependent inhibition of virus production by both mAbs in both cell types relative to the control (untreated) cells (**Fig. 6A, B**). The isotype control antibody left the infection unchanged (data not shown).

Importantly, much less if any inhibition was observed when the virus strains were preincubated, at the same conditions, with the ACHAs prior to infection (Fig. 6C, D).

ACHAs interfere mostly with the attachment phase of HIV-1 infection

To reveal with which stage of HIV-1 infection (attachment/entry/budding) the ACHAs interfere, we compared their inhibitory effects under different experimental conditions (concerning antibody treatment, infection, washing, and culturing).

When ACHA was washed out from the sample after virus infection (see protocol 2 in Materials and Methods), the extent of inhibition remained the same as in case if it was not washed out from the culture after infection (**Fig. 7A**). This indicates that the postinfection presence of ACHAs did not decrease the virus production further.

Since the level of ACHAs in the culture medium gradually declines during the relatively long assay period (Fig. 7B), we also tested if a continuous supplementation of ACHA after infection (see protocol 3 in Materials and Methods) can influence the observed inhibition. Such supplementation, however, did not result in any significant change in the final HIV-1 production (Fig. 7B), suggesting that the inhibitory effect is not coupled to inhibition of the later, budding phase.

Monoclonal ACHAs are not cytotoxic to MT-4 T and MDM cells

Finally, it was tested if the observed inhibition is due to any significant cytotoxic effect of the anticholesterol mAbs exerted on the target cells. MT-4 cells and monocyte-derived macrophages were treated with serial dilutions of ACHAs and cultured for 4 and 14 days, respectively. ACHAs proved to be nontoxic to the investigated cell types, since their survival rate remained above 90% over the whole experimental period (the cells retained both their metabolic activity and proliferation capacity) at any ACHA concentrations examined (Fig. 7C).
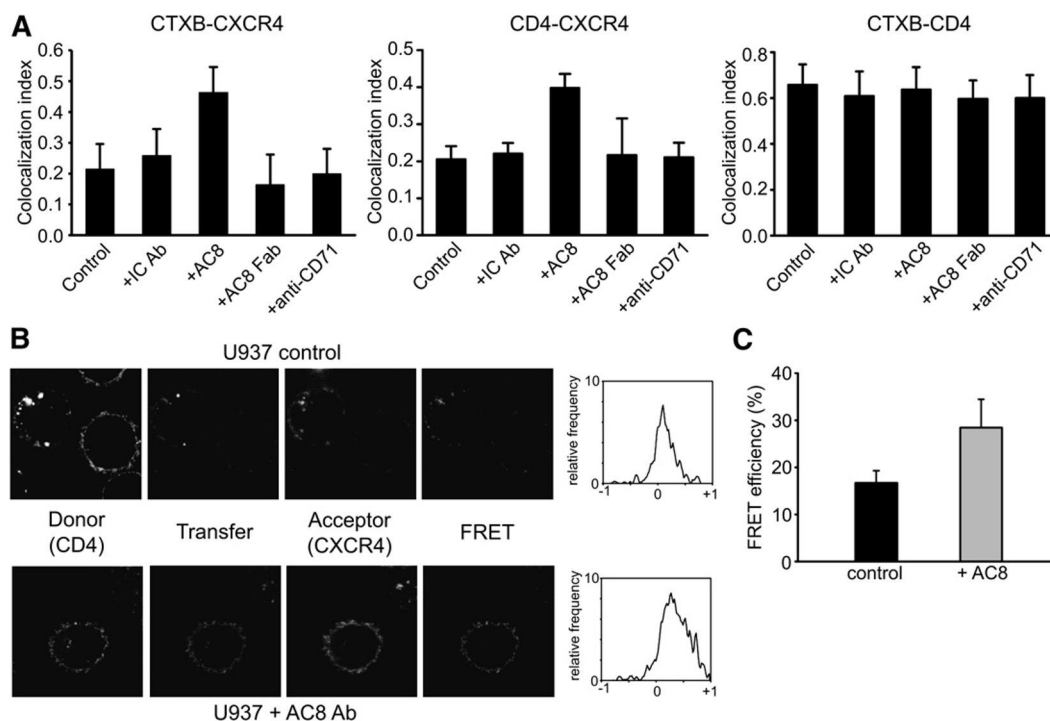
Fig. 4. AC8 substantially enhanced colocalization and FRET between CXCR4 and CD4 on human U937 macrophages. A: Colocalization indices (derived from ≥100 cells/250 regions of interest of both untreated and AC8-treated cell samples) are shown as mean ± SD for CXCR4, CD4, and CTXB in different combinations. Cells untreated or treated with AC8, isotype control Ab, Fab fragment of AC8, or anti-CD71 are displayed for comparison. B: Cells were incubated with AC8 or left untreated prior to staining with antibodies specific to CD4 and/or CXCR4. FRET measurement was carried out by confocal microscopy. Correction factors (S1, S2, S3, and S4) and factor α were calculated from only donor and only acceptor labeled samples and determined by the ImageJ RiFRET plug-in. Representative images and FRET histograms of control and AC8-treated cells are shown, respectively. FRET efficiency between CD4 and CXCR4, derived from ≥30 cells, are displayed as mean ± SD.

DISCUSSION

We report here the inhibition of HIV-1 infection/production of human monocyte-macrophage and T-cells by two new cholesterol-specific IgG antibodies, AC1 and AC8. As a novel aspect, this study points out that antilipid antibodies may act effectively not only on the virus but also on the target cell membrane, in contrast to the principle considered earlier in context of most neutralizing antibodies (26, 27).
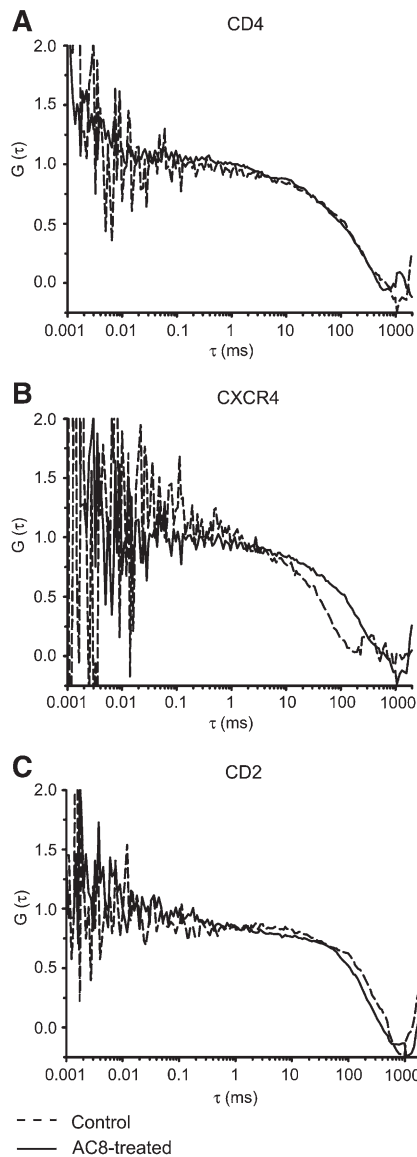
The new cholesterol-specific monoclonal antibodies bind to cholesterol- and ganglioside-rich microdomains in the membrane of various immune cells, as reported recently (2, 18). They strongly colocalize with GM_1 gangliosides as well as with GPI-anchored raft proteins (e.g., CD48 and Thy-1). Moreover, as shown here, upon binding to lipid rafts (or caveolas), these antibodies, without masking the CD4 and CXCR4 HIV-1 receptors or affecting their internalization, can remarkably remodel the plasma membrane microdomains and the spatial proximity of the above two receptor proteins.

These effects were clearly initiated by a lateral clustering (coalescence) of lipid rafts induced by binding of the mAbs to the cell surface. Cross-linking of CD71 (a nonraft protein) with mAbs was also reported to induce cell sur-

face patches, but with no overlap with GM_1 rafts (28). Since cross-linking of CD71 in our cells did not change the receptor distribution pattern, it seems that the AC8 antibody similarly to the viral gp120 (6) induces selective, cholesterol-rich raft-targeted effects on the membrane organization of HIV-1 receptors. The lack of such effect by the monovalent Fab fragment of AC8 on the target cells further confirms this notion.

Receptors and coreceptors in the cell membranes are usually not randomly distributed, and, among others, their lipid environment can also control their movement and interactions. As shown by a body of data, cholesterol is indeed required for the interaction between gp120/gp41 trimers on the surface of HIV-1 and their receptor/coreceptor counterparts on the target cells. It seems that cholesterol is a critical lipid for stabilization of raft microdomains and often of clusters of coreceptor proteins with multiple membrane-spanning helices (29), such as most, but not all chemokine receptors.

In the plasma membrane of the investigated cell types, CD4 is constitutively and highly localized, whereas CXCR4 is much more weakly raft localized. Their localization and clustering in distinct membrane microdomains on HIV-1 permissive target cells was proposed earlier (30, 31). Binding of the cholesterol-specific mAb (AC8), but not of its

TABLE 1. Translational mobility of HIV receptors on target cells assessed by FCS imaging

Epitope/Marker	Diffusion Coefficient D ± SD ($\mu m^2/s$)	
	Control	+ AC8 ACHA
CXCR4/APC-anti-CXCR4 mAb	0.17 ± 0.05* (n:26)	0.10 ± 0.02* (n:32)
CD4/Alexa 488-anti-CD4 mAb	0.10 ± 0.01 (n:22)	0.12 ± 0.03 (n:34)
CD2/Alexa 647-anti-CD2 mAb	0.15 ± 0.02 (n:23)	0.16 ± 0.03 (n:18)
Membrane cholesterol/ Alexa488-AC8	NA	0.20 ± 0.04 (n:16)

*The difference is significant between control and ACHA-treated cells ($P < 0.01$). Numbers in parentheses denote the number of cells measured. NA, not applicable.

observed in macrophages and T-cells equally (2). Although cholesterol was shown to be essential to trigger events leading to membrane fusion between the target cell and the virus, it is not required for the Env-mediated membrane fusion itself (32). Interestingly, immunization with a peptide corresponding to the caveolin-1 binding domain of gp41 virus glycoprotein was able to elicit efficient neutralizing antibodies, which act predominantly on the virus to prevent HIV-1 infection (33).

So, our view is that, in contrast to such primarily neutralizing antibodies, the cholesterol-specific antibodies may interfere mostly with the cholesterol-dependent virus-target cell interaction by modifying the membrane organization of the latter. Similarly, reorganization of ErbB membrane proteins was reported upon cross-linking of gangliosides through cholera toxin B in breast tumor cells (34). Here, we conclude that the antibodies

Fig. 5. Lateral mobility of CXCR4, but not of CD4 receptor, is markedly reduced upon AC8 mAb binding to macrophages. Cells were incubated with AC8 or left untreated prior to staining with antibodies specific to CD4 (A), CXCR4 (B), or a nonraft protein CD2 (C), and the lateral mobility of the molecules at 22°C was monitored by FCS imaging. Figures show representative fluorescence autocorrelation curves for CD4, CXCR4, and CD2 in control/untreated (dashed line) and AC8-treated cells (solid line), respectively.

Fab fragment, to the cells increased both CD4-CXCR4 co-localization and the raft association of CXCR4 by ∼2-fold. These observations, confirmed by FRET data, together suggest a view that ACHAs may induce lateral clustering of cholesterol-rich lipid rafts (or caveolas) and thus modulate the interaction pattern between raft gangliosides, CD4 and CXCR4, which are all critical in membrane attachment/entry of the virus.

The cell surface targets of both the HIV-1 virus and the new ACHAs can be the caveolin⁻ and caveolin⁺ lipid rafts alike, depending on the type of HIV-1 permissive cell. A strong association of ACHA with these microdomains was
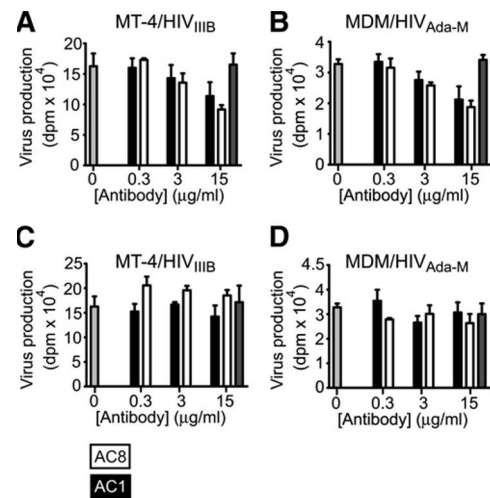

Fig. 6. Monoclonal ACHAs substantially inhibit in vitro HIV production of human T-cells and macrophages. MT-4 cells (A, C) and MDM cells (B, D) were infected with IIIB and Ada-M strains of HIV-1, respectively. Either the cells (A, B) or the viruses (C, D) were incubated with different concentrations of monoclonal ACHAs (black columns for AC1 and white columns for AC8) or left untreated (gray columns) for 1 h, prior to virus infection (see protocol 1 in Materials and Methods). Virus production, measured by RT assay, is displayed in dpm units as mean ± SD (from three independent measurements).
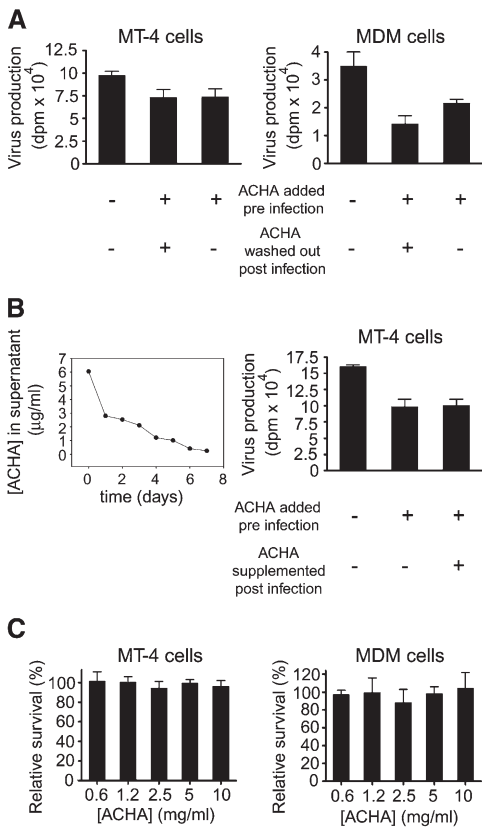
Fig. 7. The presence of ACHAs postinfection is not required for the inhibition and the antibodies are not cytotoxic. The virus production under different conditions (see protocols 2 and 3 in Materials and Methods) is shown in panels A and B. A: MT-4 cells and MDM cells were infected with IIIB and Ada-M strains of HIV-1, respectively. Monoclonal ACHAs were either not added to the cells (left columns), were preincubated with the cells and washed out (middle columns), or not washed out (right columns) after viral infection. B: ACHA level decreased in the culture supernatant of MT-4 cells postinfection as assessed by ELISA. MT-4 cells in the absence (left column) or presence (middle and right columns) of ACHA were infected with HIV-1. In order to maintain a constant level of ACHA (5 µg/ml) postinfection, the culture medium was continuously supplemented with the Ab (right column). Virus production, measured by RT assay, is displayed in dpm units as mean ± SD from three independent measurements. C: Viability of MT-4 cells and MDM cells treated with serially diluted concentrations of ACHA was determined after the whole assay period by Cell Titer assay and displayed as survival percentages (calculated from triplicates of cell samples). Viability of the untreated target cells was taken as 100%.

restrict somehow CXCR4 mobility and seemingly bring together the two critical HIV-1 receptor proteins into the same membrane microdomain, resulting in a crowding of these proteins. This may prevent attachment of the virus by "pulling together the carpet" necessary for multiple binding of viral glycoproteins to the surface of target cells.

The lateral diffusion properties of the molecules involved in HIV-1 entry, i.e., cholesterol, CD4, and CXCR4, gave further support to this view. The AC8 antibody bound to membrane cholesterol diffused moderately and strongly slower than small fluorescent cholesterol probes in model membranes with high cholesterol content or the same probes in fluid membrane phases, respectively (25). The size of the antibody label may partly be responsible for these differences. However, since the diffusion of membrane cholesterol is mostly controlled by the membrane environment rather than the extracellular aqeous phase (where the antibody is located), the slower diffusion also indicates that the AC8 cholesterol complexes diffuse in large, cholesterol-enriched microdomains.

In untreated control cells, the HIV-1 receptor CD4 diffused slower than the nonraft membrane protein CD2, and the diffusional rate of CXCR4 was significantly higher than that of CD4. The lateral mobility of CXCR4 but not of CD4 decreased substantially upon AC8 binding. The selectivity of AC8 effect on CXCR4 mobility is also demonstrated by the unaffected mobility of CD2 nonraft protein on the same cells. These data, and the similarity in diffusion coefficients of CD4 and CXCR4 after AC8 binding, are consistent with the picture that AC8 colocalizes the chemokine receptor and CD4 into the same compartment.

Based on these substantial changes in the dynamic membrane organization of HIV-1 receptors, it is postulated
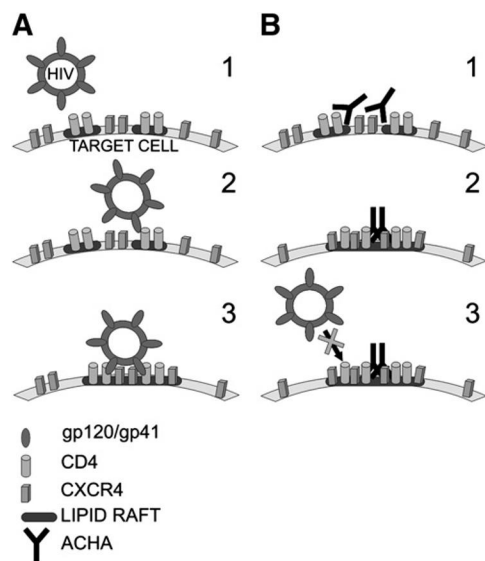
Fig. 8. A schematic model of the interference between ACHAs and HIV-1 attachment to T-cells and macrophages. A: HIV-1 enters the target cells through cholesterol-enriched membrane microrodomains (lipid rafts or caveolas). Interactions between viral glycoprotein, gp120, and raft-associated CD4 molecules result in conformational changes in gp120/gp41. Then, recruitment of CXCR4 chemokine receptors into the lipid rafts, near CD4-gp120 complexes, enables interactions of gp120 with coreceptors and formation of multimolecular complexes, resulting in attachment and internalization. B: Binding to HIV-1 permissive cells, the monoclonal cholesterol-specific IgG antibodies (ACHAs) cross-link smaller microdomains, and remodel the HIV-1 receptor-coreceptor interaction pattern. Molecular crowding of the receptors/coreceptors into the same larger microdomain may prevent a proper spatial juxtaposition of viral glycoproteins (gp120/gp41) to CD4 and chemokine receptors, necessary for formation of supramolecular complexes essential for HIV internalization. This may lead to inhibition of the viral attachment/entry.

that the AC8 mAb can mimic the action of viral glycoprotein gp120 in terms of coaggregating HIV-1 receptors and coreceptors, as proposed earlier (12). These data also concur with the findings that gp120-CD4 engagement leads to a cholesterol-sensitive lateral redistribution of membrane microdomains and a subsequent assembly of the virus internalization complex (6).

The novel cholesterol-specific antibodies preincubated with the target cells showed a significant and dose-dependent inhibitory effect on HIV-1 infection. This inhibition might be dependent on cell type, the nature of the virus strain, and the assay conditions. The inhibitory effects of AC1 and AC8 cholesterol-specific antibodies on MDM and T-cells were comparable to those previously reported for antiphosphatidylinositol-4-phosphate antibody exhibiting neutralizing activity and blocking infection of PBMC by two primary isolates of HIV-1 and to the well-known broadly neutralizing 4E10 on PBMC (13).

Considering that washing out of ACHAs prior to (or after) infection or their continuous supplementation throughout culturing did not significantly affect the final HIV-1 production, we concluded that their inhibitory effect is mostly due to modulation of the attachment/entry phase. Although it is difficult to distinguish between these two possibilities based on the present data, the unchanged inhibition observed after immediate washing out of ACHAs after infection suggests that the most likely phase that is inhibited is the attachment/anchorage of the virus to the target cell surface.

Thus, the presented data unequivocally show that the ACHAs act predominantly on the target cell membrane. Furthermore, the inhibition was found not to be due to either a direct, steric, masking effect of ACHAs or to their effects on chemokine receptor internalization. It still remains a question why the ACHAs did not act on the virus, although the viral membrane also contains cholesterol. This can be due, in part, to an insufficient extent of viral membrane-cholesterol clustering or a highly shielded epitope by surrounding viral glycoproteins.

The findings presented here may have an impact on the future development of HIV-1 specific vaccines as well (26). Recent data indicate that antibodies with membrane-pattern binding characteristics versus antibodies binding to one lipid or one protein may offer a better perspective to develop new, efficient vaccine candidates (35). The novel cholesterol-specific antibodies, recognizing "properly clustered membrane cholesterol only", seem useful to investigate the eventual role of cholesterol in the process of virus entry, which may be the Achilles' heel of the virion (36). Induction of broadly neutralizing antibodies is an essential prerequisite of an effective anti-HIV-1 vaccine. Although several different promising approaches have been applied in development of such vaccines against different viral proteins, this task seems to be extremely difficult. Therefore, alternative approaches for interfering with HIV-1 entry to target cells utilizing drugs or antibodies against cellular structures (CD4, CCR5, CXCR4, HLA class I and II, and ICAM-1) involved in the entry process (37) seem to be equally important. Since, as detailed above,

cholesterol also has a major role in these processes, cholesterol-specific antibodies may also merit consideration.

In conclusion, the new cholesterol-specific mAbs, AC1 and AC8, inhibit HIV-1 production of human T-cells and macrophages by acting on the plasma membrane and HIV-1 receptors of target cells (**Fig. 8**), and not on the virus, as most known neutralizing antibodies do. They interfere most likely with the virus attachment. Although some mechanistic details of their action on target cells remain open, we believe that the inhibitory effect and the basic background mechanisms described herein may be helpful in further studies to clarify the cholesterol dependence of the attachment/entry mechanism, as well as may serve as a molecular basis for the development of new, combined lipid raft-oriented approaches in HIV-1 therapy (26).

REFERENCES

1. Alving, C. R., and N. M. Wassef. 1999. Naturally occurring antibodies to cholesterol: a new theory of LDL cholesterol metabolism. *Immunol. Today.* **20:** 362–366.
2. Biro, A., L. Cervenak, A. Balogh, A. Lorincz, K. Uray, A. Horvath, L. Romics, J. Matko, G. Fust, and G. Laszlo. 2007. Novel anticholesterol monoclonal immunoglobulin G antibodies as probes and potential modulators of membrane raft-dependent immune functions. *J. Lipid Res.* **48:** 19–29.
3. Matko, J., and J. Szollosi. 2005. Regulatory aspects of membrane microdomain (raft) dynamics in live cells. *In* Membrane Microdomain Signaling: Lipid Rafts in Biology and Medicine. M. P. Mattson, editor. Humana Press, Totowa, NJ. 15–46.
4. Pike, L. J. 2003. Lipid rafts: bringing order to chaos. *J. Lipid Res.* **44:** 655–667.
5. Hug, P., H. M. Lin, T. Korte, X. Xiao, D. S. Dimitrov, J. M. Wang, A. Puri, and R. Blumenthal. 2000. Glycosphingolipids promote entry of a broad range of human immunodeficiency virus type 1 isolates into cell lines expressing CD4, CXCR4, and/or CCR5. *J. Virol.* **74:** 6377–6385.
6. Manes, S., G. del Real, R. A. Lacalle, P. Lucas, C. Gomez-Mouton, S. Sanchez-Palomino, R. Delgado, J. Alcami, E. Mira, and A. C. Martinez. 2000. Membrane raft microdomains mediate lateral assemblies required for HIV-1 infection. *EMBO Rep.* **1:** 190–196.
7. Nisole, S., B. Krust, and A. G. Hovanessian. 2002. Anchorage of HIV on permissive cells leads to coaggregation of viral particles with surface nucleolin at membrane raft microdomains. *Exp. Cell Res.* **276:** 155–173.
8. Fantini, J., N. Garmy, R. Mahfoud, and N. Yahi. 2002. Lipid rafts: structure, function and role in HIV, Alzheimer's and prion diseases. *Expert Rev. Mol. Med.* **4:** 1–22.
9. Jolly, C., and Q. J. Sattentau. 2005. Human immunodeficiency virus type 1 virological synapse formation in T cells requires lipid raft integrity. *J. Virol.* **79:** 12088–12094.
10. Nguyen, D. H., and J. E. Hildreth. 2000. Evidence for budding of human immunodeficiency virus type 1 selectively from glycolipid-enriched membrane lipid rafts. *J. Virol.* **74:** 3264–3272.
11. Popik, W., T. M. Alce, and W. C. Au. 2002. Human immunodeficiency virus type 1 uses lipid raft-colocalized CD4 and chemokine receptors for productive entry into CD4(+) T cells. *J. Virol.* **76:** 4709–4722.
12. Nguyen, D. H., B. Giri, G. Collins, and D. D. Taub. 2005. Dynamic reorganization of chemokine receptors, cholesterol, lipid rafts, and adhesion molecules to sites of CD4 engagement. *Exp. Cell Res.* **304:** 559–569.
13. Brown, B. K., N. Karasavvas, Z. Beck, G. R. Matyas, D. L. Birx, V. R. Polonis, and C. R. Alving. 2007. Monoclonal antibodies to

phosphatidylinositol phosphate neutralize human immunodeficiency virus type 1: role of phosphate-binding subsites. *J. Virol.* **81:** 2087–2091.

14. Adamczyk, M., J. C. Gebler, and J. Wu. 2000. Papain digestion of different mouse IgG subclasses as studied by electrospray mass spectrometry. *J. Immunol. Methods.* **237:** 95–104.

15. Costes, S. V., D. Daelemans, E. H. Cho, Z. Dobbin, G. Pavlakis, and S. Lockett. 2004. Automatic and quantitative measurement of protein-protein colocalization in live cells. *Biophys. J.* **86:** 3993–4003.

16. Roszik, J., D. Lisboa, J. Szollosi, and G. Vereb. 2009. Evaluation of intensity-based ratiometric FRET in image cytometry - approaches and a software solution. *Cytometry A.* **75:** 761–777.

17. Haustein, E., and P. Schwille. 2007. Fluorescence correlation spectroscopy: novel variations of an established technique. *Annu. Rev. Biophys. Biomol. Struct.* **36:** 151–169.

18. Gombos, I., G. Steinbach, I. Pomozi, A. Balogh, G. Vamosi, A. Gansen, G. Laszlo, G. Garab, and J. Matko. 2008. Some new faces of membrane microdomains: a complex confocal fluorescence, differential polarization, and FCS imaging study on live immune cells. *Cytometry A.* **73:** 220–229.

19. Gendelman, H. E., J. M. Orenstein, M. A. Martin, C. Ferrua, R. Mitra, T. Phipps, L. A. Wahl, H. C. Lane, A. S. Fauci, D. S. Burke, et al. 1988. Efficient isolation and propagation of human immunodeficiency virus on recombinant colony-stimulating factor 1-treated monocytes. *J. Exp. Med.* **167:** 1428–1441.

20. Wong-Staal, F., G. M. Shaw, B. H. Hahn, S. Z. Salahuddin, M. Popovic, P. Markham, R. Redfield, and R. C. Gallo. 1985. Genomic diversity of human T-lymphotropic virus type III (HTLV-III). *Science.* **229:** 759–762.

21. Hoffman, A. D., B. Banapour, and J. A. Levy. 1985. Characterization of the AIDS-associated retrovirus reverse transcriptase and optimal conditions for its detection in virions. *Virology.* **147:** 326–335.

22. Zhao, Q., J. T. Ernst, A. D. Hamilton, A. K. Debnath, and S. Jiang. 2002. XTT formazan widely used to detect cell viability inhibits HIV type 1 infection in vitro by targeting gp41. *AIDS Res. Hum. Retroviruses.* **18:** 989–997.

23. Rey, M., A. Valenzuela-Fernandez, A. Urzainqui, M. Yanez-Mo, M. Perez-Martinez, P. Penela, F. Mayor, Jr., and F. Sanchez-Madrid. 2007. Myosin IIA is involved in the endocytosis of CXCR4 induced by SDF-1alpha. *J. Cell Sci.* **120:** 1126–1133.

24. Xiao, X., L. Wu, T. S. Stantchev, Y. R. Feng, S. Ugolini, H. Chen, Z. Shen, J. L. Riley, C. C. Broder, Q. J. Sattentau, et al. 1999. Constitutive cell surface association between CD4 and CCR5. *Proc. Natl. Acad. Sci. USA.* **96:** 7496–7501.

25. Bacia, K., P. Schwille, and T. Kurzchalia. 2005. Sterol structure determines the separation of phases and the curvature of the liquid-ordered phase in model membranes. *Proc. Natl. Acad. Sci. USA.* **102:** 3272–3277.

26. Alving, C. R., Z. Beck, N. Karasavva, G. R. Matyas, and M. Rao. 2006. HIV-1, lipid rafts, and antibodies to liposomes: implications for anti-viral-neutralizing antibodies. *Mol. Membr. Biol.* **23:** 453–465.

27. Haynes, B. F., J. Fleming, E. W. St Clair, H. Katinger, G. Stiegler, R. Kunert, J. Robinson, R. M. Scearce, K. Plonk, H. F. Staats, et al. 2005. Cardiolipin polyspecific autoreactivity in two broadly neutralizing HIV-1 antibodies. *Science.* **308:** 1906–1908.

28. Harder, T., P. Scheiffele, P. Verkade, and K. Simons. 1998. Lipid domain structure of the plasma membrane revealed by patching of membrane components. *J. Cell Biol.* **141:** 929–942.

29. Charrin, S., S. Manie, C. Thiele, M. Billard, D. Gerlier, C. Boucheix, and E. Rubinstein. 2003. A physical and functional link between cholesterol and tetraspanins. *Eur. J. Immunol.* **33:** 2479–2489.

30. Kozak, S. L., J. M. Heard, and D. Kabat. 2002. Segregation of CD4 and CXCR4 into distinct lipid microdomains in T lymphocytes suggests a mechanism for membrane destabilization by human immunodeficiency virus. *J. Virol.* **76:** 1802–1815.

31. Singer, I. I., S. Scott, D. W. Kawka, J. Chin, B. L. Daugherty, J. A. DeMartino, J. DiSalvo, S. L. Gould, J. E. Lineberger, L. Malkowitz, et al. 2001. CCR5, CXCR4, and CD4 are clustered and closely apposed on microvilli of human macrophages and T cells. *J. Virol.* **75:** 3779–3790.

32. Viard, M., I. Parolini, M. Sargiacomo, K. Fecchi, C. Ramoni, S. Ablan, F. W. Ruscetti, J. M. Wang, and R. Blumenthal. 2002. Role of cholesterol in human immunodeficiency virus type 1 envelope protein-mediated fusion with host cells. *J. Virol.* **76:** 11584–11595.

33. Hovanessian, A. G., J. P. Briand, E. A. Said, J. Svab, S. Ferris, H. Dali, S. Muller, C. Desgranges, and B. Krust. 2004. The caveolin-1 binding domain of HIV-1 glycoprotein gp41 is an efficient B cell epitope vaccine candidate against virus infection. *Immunity.* **21:** 617–627.

34. Nagy, P., G. Vereb, Z. Sebestyen, G. Horvath, S. J. Lockett, S. Damjanovich, J. W. Park, T. M. Jovin, and J. Szollosi. 2002. Lipid rafts and the local density of ErbB proteins influence the biological role of homo- and heteroassociations of ErbB2. *J. Cell Sci.* **115:** 4251–4262.

35. Beck, Z., N. Karasavvas, G. R. Matyas, and C. R. Alving. 2008. Membrane-specific antibodies induced by liposomes can simultaneously bind to HIV-1 protein, peptide, and membrane lipid epitopes. *J. Drug Target.* **16:** 535–542.

36. Haynes, B. F., and S. M. Alam. 2008. HIV-1 hides an Achilles' heel in virion lipids. *Immunity.* **28:** 10–12.

37. Phogat, S., R. T. Wyatt, and G. B. Karlsson Hedestam. 2007. Inhibition of HIV-1 entry by antibodies: potential viral and cellular targets. *J. Intern. Med.* **262:** 26–43.